High-resolution temporal variations of nitrate in a high-elevation pond in alpine tundra (NW Italian Alps)

High-resolution temporal variations of nitrate in a high-elevation pond in alpine tundra (NW Italian Alps)

N. Colombo[a,b,c], R. Balestrini[d], D. Godone[e,c*], D. Vione[f,c], D. Said-Pullicino[a], G. Viviano[d], M. Martin[a], C.A. Delconte[d], S. Fratianni[g,c], A.G. Capodaglio[h], E. Pintaldi[a], M. Freppaz[a,c], F. Salerno[d,i]

[a]University of Turin, Department of Agricultural, Forest and Food Sciences, Grugliasco, Italy

[b]CNR-IRSA (National Research Council - Water Research Institute), Rome, Italy

[c]Research Center on Natural Risk in Mountain and Hilly Environments, NatRisk, University of Turin, Grugliasco, Italy

[d]CNR-IRSA (National Research Council - Water Research Institute), Brugherio, Italy

[e]CNR-IRPI (National Research Council - Research Institute for Geo-Hydrological Protection), Turin, Italy

[f]University of Turin, Department of Chemistry, Turin, Italy

[g]University of Turin, Department of Earth Sciences, Turin, Italy

[h]University of Pavia, Department of Civil Engineering and Architecture, Pavia, Italy

[i]CNR-ISP (National Research Council - Institute of Polar Sciences), Venezia Mestre (VE), Italy

Correspondence to: danilo.godone@irpi.cnr.it (D. Godone)

Abstract

High-resolution temporal measurements in remote, high-elevation surface waters are required to better understand the dynamics of nitrate (NO_3^-) in response to changes in meteoclimatic conditions. This study reports on the first use of a UV–Vis submersible spectrophotometric probe (UV–Vis probe) to measure the hourly concentration of nitrate nitrogen (NO_3^--N) in a pond located at 2722 m a.s.l. in an alpine tundra area (NW Italian Alps), during two snow-free seasons (July–October) in 2014 and 2015. Weekly analyses of NO_3^--N and stable isotopes of water ($\delta^{18}O$ and $\delta^{2}H$), together with continuous meteorological, water temperature and turbidity measurements, were performed over the same period. The integration of in-situ UV–Vis spectrophotometric measurements and weekly samples allowed depicting the role of summer precipitation, snow melt, and temperature (air and water) in influencing NO_3^- dynamics. Short-duration meteorological events (e.g., summer storms and rain-on-snow events) produced rapid variations of in-pond NO_3^-

concentration, i.e., fivefold increase in 18 hours, that would not be detectable using the traditional manual collection of discrete samples. The observed seasonal variability of NO_3^- concentration, negatively correlated with water temperature, highlighted the important role of in-pond biological processes leading to an enhanced N uptake and to the lowest NO_3^- concentration in the warmer periods. The occurrence of heavy rainfall events critically altered the expected seasonal NO_3^- trends, increasing the N supply to the pond. The comparison of N dynamics in two years characterised by extremely different meteoclimatic conditions allowed to obtain insights on the potential effects of climate changes (e.g., high air temperature, heavy rainfalls, and rain-on-snow events) on sensitive aquatic ecosystems as high-elevation ponds.

Keywords: NO_3^-, surface water, mountains, LTER, turbidity, N retention

1 Introduction

Changes in climate and nutrient input can have strong effects on mountain ecosystems, in particular on those located above the tree line, in alpine tundra (Balestrini et al., 2013). These ecosystems are susceptible to alterations that affect their physical structure and biological communities, because of their complex topography, harsh climate, long-lasting snow cover, and a short growing season (Williams et al., 2002; Balestrini et al., 2013; Barnes et al., 2014). These extreme environments are key components of the water cycle and are integral parts of the so called "water towers", referring to the role of mountains as providers of essential freshwater to lowland areas (Viviroli et al., 2007, 2020).

In this context, high-elevation lakes play an important role in the hydrological and chemical dynamics of mountain watersheds (Catalan et al., 2006; Tartari et al., 2008; Tolotti et al., 2009; Salerno et al., 2016a). The general lack of direct human influence on these lakes and the fact that their physical, chemical and biological properties respond rapidly to climate-related changes make them key freshwater reference sites for global scale processes (Adrian et al., 2009; Mladenov et al., 2009; Salerno et al., 2016b; Rogora et al., 2020). In addition, water bodies located in high-elevation environments are generally characterised by small size, and can be defined as ponds (area $< 2 \times 10^4$ m^2; Hamerlík et al., 2014). The relatively low water volumes and high surface area to depth ratios make these water bodies even more fragile and sensitive to environmental changes (Hamerlík et al., 2014).

Chronic, relatively high, inputs of nitrogen (N) from atmospheric deposition can, over time, saturate the N assimilation capacity of biological processes in remote, commonly, N-limited ecosystems (N saturation, see Aber et al., 1998). The effects of N-saturation are complex with impact on both terrestrial and aquatic ecosystems, and include the enhanced leaching of inorganic N from soils to surface waters (Balestrini et al., 2006; Rogora et al., 2012). In this regard, nitrate (NO_3^-) has been investigated due to its role in affecting the productivity and species diversity in

remote mountain waters (Elser et al., 2009; Slemmons et al., 2017). In mountain catchments, NO_3^- dynamics in surface waters depend on several drivers, such as land-cover and topographic characteristics (slope and presence of soil, bedrock, and cryospheric elements; e.g., Kopáček et al., 2005; Balestrini et al., 2013; Colombo et al., 2019a), climatic conditions (e.g., precipitation, snow-cover duration, and air temperature; e.g., Kopáček et al., 2005; Williams et al., 2015a,b; Freppaz et al., 2019), and anthropogenic activities (e.g., N deposition from atmospheric pollution; Elser et al., 2009; Rogora et al., 2012). Meteo-hydrological events such as snowmelt and summer storms, able to generate rapid changes in water flow paths, nutrient source areas, and biogeochemical processes, can strongly affect NO_3^- concentrations and fluxes in mountain surface waters (Williams et al., 2002; Clow et al., 2003; Sickman et al., 2003; Williams et al., 2007; Sebestyen et al., 2008). However, little work has been done to characterise the hydrochemical response, with particular reference to NO_3^-, to meteorological events in ponds and lakes located above the treeline. Furthermore, the biological in-stream/lake processes are often ignored in alpine catchments, although a growing body of literature demonstrates that they are important regulators of nutrient retention and export in headwater catchments (Mulholland et al., 2006; Roberts and Mulholland, 2007; Rusjan and Mikoš, 2010)

Studies focusing on NO_3^- dynamics in remote surface waters generally rely on manual collection of discrete samples and subsequent laboratory analysis (e.g., Williams et al., 2007; Vione et al., 2021). This approach is expensive, time-consuming, and is often affected by intrinsic risks associated with extreme weather conditions and location (e.g., orographic thunderstorms, rockfalls, snow avalanches, ice falls, etc.), resulting in sporadic and/or low temporal-resolution data sets. For this reason, essential insights into the processes occurring in these ecosystems are lacking or incomplete, especially the ones occurring on short time scales (hours, days, or even weeks).

High-resolution in-situ measurements could refine the assessment of nutrient fluxes and temporal dynamics of high-elevated aquatic ecosystems, in turn improving the understanding of how weather- and climate-driven modifications could impact these fragile and rapidly changing

ecosystems. To do this, in situ sensors can be deployed in remote and hardly accessible locations where repeated, grab sampling techniques would be logistically difficult and potentially dangerous (e.g., Beaton et al., 2017). Ultraviolet–visible light (UV–Vis) spectrophotometers are currently available to evaluate variations in NO_3^- concentrations in surface waters with high temporal resolution. Research has focused on the use of similar sensors especially in running waters in lowland areas (e.g., Pellerin et al., 2012; Burns et al., 2019); however, applications of in-situ UV–Vis spectrophotometers in remote, high-elevation water bodies have not yet been reported.

In the present work, a UV–Vis spectrophotometer was installed and used to monitor nitrate nitrogen (NO_3^--N) concentration and turbidity in the Col d'Olen Rock Glacier Pond (2722 m a.s.l.) located in the NW Italian Alps, during the summers 2014 and 2015. In addition, grab samples were collected on a weekly basis and analysed for NO_3^--N concentration and isotopic composition of water ($\delta^{18}O$ and $\delta^{2}H$). Finally, meteorological parameters (air temperature, rainfall, and snow depth) and water temperature were continuously measured during the investigated period. The Col d'Olen Rock Glacier Pond was selected as a model system for this investigation since the hydrochemical features of the pond have been deeply studied in the last years to understand the influence of a rock glacier flowing into the pond (Colombo et al., 2018a,b, 2019a, 2020). This provided a solid knowledge baseline for interpreting the high-temporal-resolution data obtained in this work.

The aim of this study was to unravel the mechanisms underlying the dynamics of nitrate during seasonal transitions and short-lived meteorological events in a remote, high-elevation pond. The implications of our findings on the effect of climate change on N cycle were also discussed.

2 Materials and Methods

2.1 Study area

The research site (Angelo Mosso Scientific Institute site) is a node of the Long-Term Ecological Research (LTER) network in Italy, situated in the North-Western Italian Alps, at the boundary

between Valle d'Aosta and Piemonte regions (Fig. 1a). The Col d'Olen Rock Glacier Pond is situated at the Col d'Olen Rock Glacier terminus (Fig. 1b,c), at an elevation of 2722 m a.s.l. Its catchment area is approximately 206,000 m^2 (Fig. 1b). The pond has an area of ca. 1600 m^2 (covering 0.8 % of the catchment), with maximum length and width of ca. 60 × 40 m, and reaches a maximum depth of about 3 m (average depth: 1.8 m). It is a low-turbidity water pond, characterised by ultraoligotrophic conditions and by the lack of macroalgal and macrophyte cover at the bottom (Mania et al., 2019). Two water temperature profiles were performed in the pond on 12 July and 6 September 2015, showing a slight temperature decrease toward the bottom (300 cm depth) of 0.9 °C and 0.8 °C, respectively (Colombo et al., 2018a). A thick layer (up to several decimetres) of fine-grained sediments covers the bottom of the pond (Sambuelli et al., 2015; Colombo et al., 2020). Coarse sediment constitutes the main land cover in the pond catchment, followed by bedrock outcrops; vegetated soil is also present, especially in the pond surroundings (Colombo et al., 2019a). More details on the catchment structural setting, hydrological and chemical dynamics, and ecosystem features of the pond can be found in Colombo et al. (2018a,b; 2019a; 2020) and Mania et al. (2019).

According to recent climate data series (2008–2015) obtained by the Col d'Olen AWS (Automatic Weather Station, Meteomont Service, Italian Army, 2900 m a.s.l., located approx. 900 m from the pond), the area is characterised by 400 mm of rainfall (on average) during the summer season, a mean annual air temperature of –2.6 °C, and a mean cumulative snowfall of 850 cm. The snowpack generally develops by late October to early November, and melt out usually occurs in July. At the site, heavy (> 10 mm) and very heavy (> 20 mm) rainfall events are relatively frequent during the snow-free season (Freppaz et al., 2019). At the site, mean annual nitrate concentrations in snow and rain are 5 and 10 µmol L^{-1}, respectively (year 2015, Colombo et al., 2019a).

2.2 Meteorological measurements

Air temperature and snow depth were measured at the Col d'Olen AWS. Rain data were obtained from the Gressoney-La-Trinité - Lago Gabiet AWS (2379 m a.s.l., managed by Regione Autonoma Valle d'Aosta), located ca. 2.5 km from the pond; the use of the Gressoney-La-Trinité - Lago Gabiet AWS was due to some data gaps in the precipitation data of the Col d'Olen AWS during the analysed time-span. Data were acquired on an hourly basis.

2.3 Spectroscopic and water temperature measurements

A UV–Vis submersible spectrophotometric probe (s::can sprectro::lyser^{TM}, s::can Messtechnik GmbH, Austria; Fig. 1d) was used for high-resolution spectroscopic measurements in the pond. The deployed probe had a measuring path length of 35 mm, suggested by the manufacturer for use in natural water. The probe measured absorbance over a 200–730 nm range at 2.5 nm intervals, thus it is potentially able to monitor concentrations of all compounds which generate an absorption. In particular, nitrate nitrogen (NO_3^--N) induces an absorption between 210 and 240 nm (UV range) and turbidity between 400 and 700 nm (Visible range). Although NO_3^--N can be estimated by the probe using the manufacturer's default global calibration (Langergraber et al., 2003), a local calibration algorithm can also be used to adapt the global calibration to the local conditions (Fleischmann et al., 2001). Local calibration uses laboratory analysis on actual samples from the investigated medium (Fleischmann et al., 2001), to account for matrix effects. To properly perform the local calibration, a sufficient number of water samples should be collected onsite prior to the deployment of the instrument, to cover the entire expected range of possible NO_3^--N concentrations. In our case, considering the remoteness of the study area and the scarce availability of enough existing grab samples covering the whole range of nitrate concentrations (which is a typical condition encountered by researchers in these kind of high-elevation settings), the default global calibration was used (detection range: 0.35–715 µmol L^{-1}; Snazelle, 2015).

The reduced size of the probe (length: 58 cm, diameter: 4.4 cm, weight: ca. 2 kg) made this instrument particularly suitable for installation in remote areas. The probe was installed at the southern side of the pond (Fig. 1c), approximately 3-m in from the shoreline (Fig. 1e) and at ca. 1-m depth. The sensor was installed in a zone of the pond not directly influenced by the rock glacier, thus representative of the processes ongoing in the entire pond and its catchment (Colombo et al., 2018a,b). The sensor was placed in horizontal position close to the pond bottom, with bottom-facing measuring path to avoid direct solar radiation incidence, prevent particles sedimentation in the measuring window, and avoid adhesion of gas bubbles. Power was provided by a 12 V / 18 Ah battery charged by a solar panel (Fig. 1f) that ensured continuous measurements during the monitoring period. In addition, the measuring window was automatically cleaned at 3-hour intervals using pressurised air (Fig. 1g). Data were acquired at 3-hour intervals over the periods 14 July – 9 October 2014 (88 days) and 29 June – 31 July 2015 (33 days). The probe was removed on 9 October 2014 to prevent damages to the installation due to ice formation on the pond surface. On 1 August 2015, a sensor malfunction occurred due to a thunderstorm, preventing its recovery and thus further measurements during the remaining summer 2015 campaign. Raw data were saved in an internal datalogger. Every two weeks the probe was checked for its operational conditions and no technical issues were found.

Several processes are capable of influencing the performance of UV–Vis probes in estimating nitrate concentrations. For instance, interference of pH and salinity on nitrate quantification might occur (cf., Edwards et al., 2001), however, pH and electrical conductivity at the Rock Glacier Pond during the investigated period were between 7 and 7.5 and 32 and 45 μS cm^{-1}, respectively (Colombo et al., 2018b), thus any interference was excluded. Also, since NO_2^--N concentrations in pond water were extremely low, generally below the detection limits (Colombo et al., 2018b), an interference effect of nitrite could be excluded too (Huebsch et al., 2015). Furthermore, the probe internal algorithm compensates for the effect of turbidity, thus from this point of view any relevant interference could be discarded. Finally, water temperature might also have an effect on nitrate

concentration estimation (Pellerin et al., 2012), however, during a comparison test between several probes for measuring nitrate, no relevant drift was observed for a probe like the one used in the present study (Snazelle, 2015). Thus, the conditions of the pond and the characteristics of the employed UV–Vis probe were considered suitable for estimating the NO_3^--N temporal variations in our setting.

Water temperature in the pond was measured continuously (at 3-hour intervals) from 28 July to 9 October 2014 and from 29 June to 12 October 2015 by means of a miniature temperature Onset HOBO® TidbiT v2 Temp logger (accuracy ±0.21 °C, resolution 0.02 °C) installed at the pond bottom close to the probe.

2.4 Water level and grab samples collection and analysis

Water level was measured approximately on a weekly basis using a hydrometric station with direct observations from 14 July to 9 October 2014 and from 29 June to 12 October 2015. In conjunction with the water level measurements, the pond was sampled using a telescopic sampling pole, collecting samples close to the probe site (13 samples in 2014 and 15 samples 2015), approximately at the same depth as the probe. To validate the probe during its deployment period, sample collection was performed at the exact time of the probe measurement to properly compare sample analyses with the instantaneous probe data (13 samples in 2014 and 5 samples in 2015).

Water samples for NO_3^--N analyses were collected in new polyethylene tubes (volume 50 mL). To properly choose the tubes used for the sampling, they were preliminarily tested by storing Milli-Q water in conditions similar to those of the samples; no release of NO_3^--N was detected. The content of the tubes was immediately filtered in the field through a 0.2 µm nylon membrane filter. Given the expected low NO_3^--N concentrations, the suitability of the filters for our analyses was also tested; several filtered blank experiments were performed and no modifications in NO_3^--N occurred. In addition, filtered blank experiments were conducted on different filters lots and filters

were tested also on calibration standards, and no anomalies were detected. Samples were stored in an ice-packed cooler during transport from the field site, and then immediately transferred to the laboratory where they were refrigerated (at +4 °C) until analysis. The concentration of NO_3^--N was determined by ion chromatography (Dionex DX-500, Sunnyvale, California, USA). Analysis quality was determined by including method blanks and repeated measurements of standard reference samples. Analytical precision was < 10% and LOD was 1 µmol L^{-1}.

Water samples for isotopic analyses were collected using new polyethylene tubes with airtight caps (volume 50 mL), completely filled to avoid head space. Furthermore, a 300 cm-deep snow profile was sampled before the melting season near the Col d'Olen AWS on 14 April 2015; six snow samples were collected at 50-cm intervals. A bulk rainwater sampler was also installed on 28 July 2014 close to the pond and sampled weekly (if precipitation occurred). Eight and four rain samples were collected in 2014 and 2015, respectively. Analysis was performed at the INSTAAR (Institute of Arctic and Alpine Research) Kiowa Environmental Chemistry Laboratory of the University of Colorado at Boulder (USA), by means of a cavity ring-down spectroscopy analyzer - Picarro L2130-i (Picarro Inc., Sunnyvale, California, USA). Isotopic composition was expressed as a δ (per mil) ratio of the sample to the Vienna Standard Mean Ocean Water (VSMOW), where δ is the ratio of $^{18}O/^{16}O$ and $^{2}H/^{1}H$. Analytical precision was 0.1 ‰ and 1 ‰ for $\delta^{18}O$ and $\delta^{2}H$, respectively.

2.5 Data elaboration and analysis

To assess the performance of the probe, NO_3^--N concentrations estimated by the probe were compared to the ones determined in 18 grab samples; then, grab sample data were used to post-calibrate the probe data, through a simple linear regression approach. In addition, the degree of correlation among selected parameters was verified through the Pearson's correlation coefficient (r), if data were normally distributed (Kolmogorov-Smirnov test; Carvalho, 2015). The non-parametric

241 Spearman's test was used if data did not follow the normal distribution, even after the application of
242 log-transformation. All analyses were performed in R environment (R Core Team, 2022).
243
244 # 3 Results
245 ## 3.1 Meteorological and hydrological conditions
246 The two investigated years showed a large difference in the snow-cover duration. Indeed, the
247 melt-out date of snow occurred at the beginning of August in 2014 (Fig. 2a), while it occurred one
248 month earlier in 2015 (Fig. 2b). The two periods differed also considering the rainfall, indeed 2014
249 was characterised by a lower cumulated amount (351 mm) with respect to 2015 (567 mm). In 2014,
250 heavy rain events mostly occurred from mid-July, when snowpack was still present, to mid-August
251 (Fig. 2a). July was the wettest month in 2014, with 154 mm of cumulated rain. Differently, in 2015,
252 most of the heavy rain events occurred in the snow-free August (Fig. 2b), which was also the
253 wettest month (303 mm). The mean daily air temperature during the investigated periods was +2.9
254 °C and +4 °C in 2014 and 2015, respectively. The range of variation was also different between the
255 two years. Indeed, daily air temperature variation in 2014 was more reduced (Fig. 2a), ranging from
256 –3.0 °C (6 October) to +8.1 °C (17 July), while in 2015 it was larger (Fig. 2b), ranging from –5.8
257 °C (1 October) to +12.1 °C (5 July).
258 Regarding the daily water temperature, in 2014, an absolute minimum value of +3.5 °C was
259 registered at the beginning of the measurement period (28 July), which was followed by a
260 progressive increase until the absolute maximum value of +10.7 °C, that was reached at the end of
261 August (31 August, Fig. 2a). Then, a decrease in water temperature occurred until the end of the
262 investigated period, reaching a minimum value of +5.7 °C (10 October). It is also worth noting a
263 short period (10 days), from the end of September to the beginning of October, when a water
264 temperature increase occurred (maximum value: +8.8 °C, 4 October, Fig. 2a). In 2015, the
265 monitored period began with a sharp water temperature increase, from +4.0 °C to +13.2 °C in 18

266 days (29 June – 17 July, Fig. 2b). The temperature remained relatively high until 6 August (absolute
267 maximum value: +13.7 °C), and then decreased to +3.9 °C in correspondence with an intense rainy
268 period (8 – 24 August). Another water temperature increase occurred at the beginning of
269 September, after which the temperature finally declined toward the end of the season (absolute
270 minimum value: +2.3 °C, 3 October), when the snowpack started building up (Fig. 2b). During the
271 deployment period of the probe, the water temperature exhibited daily cycles with the lowest mean
272 values at 09:00 AM and the highest mean values at 6:00 PM, during both years; the mean difference
273 between the highest and lowest diel values was 1.2 °C in 2014 and 0.9 °C in 2015 (not shown).
274 Regarding the water level, starting from the same initial value (about 100 cm), a level decline
275 was weekly recorded in both seasons with a minimum value measured in October, which led to an
276 overall decrease of about 30 cm (Fig. 2c,d). Despite the decreasing trend, some increases due to
277 precipitation events occurred, for instance in September 2014 (4 cm increase) and August 2015 (10
278 cm increase).
279 $\delta^{18}O$ and $\delta^{2}H$ of water molecule were used as hydrologic tracers to detect the main water sources
280 of the pond, e.g., water from snow melt and precipitation events (cf., Colombo et al., 2018b, 2019b;
281 Brighenti et al., 2021). The most depleted values were shown by snow for $\delta^{18}O$ (mean −18.9 ‰,
282 range: −22.9 to −16.2 ‰) and $\delta^{2}H$ (mean: −139.2 ‰, range: −171.2 to −116.2 ‰). On the opposite,
283 rain had the most enriched values of $\delta^{18}O$ (mean: −10.0 ‰, range: −12.3 to −7.8 ‰) and $\delta^{2}H$
284 (mean: −63.9 ‰, range: −89.3 to −46.8 ‰). Pond water values of $\delta^{18}O$ (mean: −12.8 ‰, range:
285 −14.8 to −10.4 ‰) and $\delta^{2}H$ (mean: −90.3 ‰, range: −106.9 to −70.8 ‰) arranged in between snow
286 and rain ones. A progressive isotopic enrichment occurred during the analysed periods, with some
287 evident sharp enrichments after heavy rain events in July 2014, July 2015, and August 2015 (Figs.
288 2c,d, 3). The isotope values of snow, rain, and water pond, shown in a dual isotope diagram (Fig. 3),
289 fell close to the Local Meteoric Water Line (LMWL) calculated for Northern Italy by Longinelli
290 and Selmo (2003).
291

3.2 NO_3^--N concentrations

3.2.1 Grab samples

In 2014, the highest NO_3^--N concentrations occurred at the beginning of the sampling season, in July (6.6–8.9 µmol L^{-1}), then they decreased in August (2.7–4.1 µmol L^{-1}, Fig. 2e). A slight, progressive NO_3^--N increase occurred toward the end of the sampling period, in September and October (ca. 5 µmol L^{-1}). In 2015, NO_3^--N concentrations declined from the end of June (5.6 µmol L^{-1}) toward the minimum values measured in second half of July (ca. 2 µmol L^{-1}), which were then followed by a sharp increase between the end of July and mid-August (6.2–13.8 µmol L^{-1}, Fig. 2f). After a concentration decline toward mid-September (3.7 µmol L^{-1}), NO_3^--N concentrations increased again between the end of September and the beginning of October (5.0–6.6 µmol L^{-1}).

3.2.1 UV–Vis probe measurements

The probe provided a good estimate of NO_3^--N temporal variations; indeed, the correlation coefficient (r) between grab sample and probe NO_3^--N concentrations was 0.83 ($p < 0.01$) (Fig. 4). Simple linear regression was used to post-calibrate the probe, obtaining a mean absolute percentage error of ± 18 %. The residuals of the probe vs. grab sample regression were normally distributed (Fig. 4) and did not display any temporal trend (not shown), thus confirming the good quality of the post-calibration.

The daily probe data showed that, in 2014, after a 6-day period of relatively dry conditions (14–19 July 2014; cumulated rain: 7.8 mm), during which NO_3^--N concentrations slightly declined (from 7.0 to 5.5 µmol L^{-1}), a sharp NO_3^--N increase was measured on 20–21 July 2014 (Fig. 5a,c). During these days, 3-hour data showed that 39.8 mm of rain fell in 33 hours and NO_3^--N concentrations increased from 5.6 to 11.2 µmol L^{-1} (Fig. 6a). Then, NO_3^--N remained relatively stable (ca. 8–10 µmol L^{-1}) for 8 days even though other abundant rainy events occurred (22–29 July 2014; cumulated rain: 107 mm). The following period (1–22 August) was characterised by a

317 gradual NO_3^--N decline, until reaching a plateau that lasted approximately two weeks (23 August–5
318 September), with minimum concentrations of ca. 3.0 µmol L^{-1} (Figs. 5c, 6b). After this period,
319 NO_3^--N concentrations slowly increased until 16 September (ca. +1 µmol L^{-1}), when a faster
320 increase occurred (ca. +2 µmol L^{-1} in 4 days; Figs. 5c, 6c). Again, NO_3^--N concentrations reached a
321 plateau around 5 µmol L^{-1} and then increased at the end of the season (6.5 µmol L^{-1}). Temporal
322 variations of turbidity showed similarities with NO_3^--N ones, such as higher values in July
323 (mean±st.dev.: 3.3±2.1 Formazine Turbidity Unit - FTU; Fig. 5c). From 1 August to the third week
324 of September, turbidity remained low and stable (mean±st.dev.: 0.8±0.2 FTU), while it slightly
325 increased in October (mean±st.dev.: 1.2±0.6 FTU), similarly to NO_3^--N (Fig. 5c). Turbidity was
326 significantly correlated to NO_3^--N ($r = 0.71$, $p < 0.001$, $n = 697$, 3-hour data).
327 In 2015, a dry period characterised the first investigated weeks (29 June – 21 July, cumulated
328 rain: 13.2 mm), during which daily NO_3^--N concentrations progressively decreased from 7.1 µmol
329 L^{-1} (29 June) to 3.1 µmol L^{-1} (21 July; Fig. 5b,d). After the initial dry period, a rain event occurred
330 on 22 July, with 32.2 mm of rain cumulated in 6 hours; a fivefold NO_3^--N increase occurred, with
331 3-hour concentrations that increased from 2.9 to 15 µmol L^{-1} (Figs. 5b,d, 6d). Then, a progressive
332 decrease in NO_3^--N occurred until the end of the studied period (Fig. 5d). Turbidity and NO_3^--N
333 showed similar temporal variations (Figs. 5d, 6d), indeed they were significantly correlated ($r =$
334 0.86, $p < 0.001$, $n = 260$, 3-hour data).
335 In 2014, an inverse correlation was found between 3-hour water temperatures and NO_3^--N
336 concentrations estimated by the probe ($r = –0.89$, $p < 0.001$, $n = 589$). A correlation analysis was
337 also performed between daily water temperatures and NO_3^--N concentrations in grab samples: also
338 in this case, a significant, negative correlation was found ($r = –0.74$, $p < 0.01$; $n = 11$). In 2015, no
339 significant correlation was found between 3-hour water temperatures and NO_3^--N concentrations

estimated by the probe (r = –0.01, p = 0.93; n = 260) and neither between daily water temperatures and NO_3^--N concentrations in grab samples (r = –0.57, p = 0.31; n = 5).

Finally, no evident and temporally consistent daily cycles in NO_3^--N concentrations were found during both investigated years; the mean difference between the highest and lowest diel values was 0.3 µmol L^{-1} in 2014 and 0.6 µmol L^{-1} in 2015 (not shown). However, in the first days of 2015 (29 June – 5 July), during the snow-melt phase, daily NO_3^--N amplitude reached values up to 4.1 µmol L^{-1}, with the highest concentrations (7–9 µmol L^{-1}) occurring in the evening (generally at 09:00 PM; not shown).

4 Discussion

4.1 Early summer: snow-melt period

The different temperature and snow regimes at the beginning of the summer seasons have greatly influenced the snowmelt period in the analysed years. In 2014, the sampling campaign started when snow depth was 120 cm (14 July) corresponding to ca. 30 % of the maximum snow depth while, in 2015, snow depth was 70 cm, thus 90 % of snowpack was already melted.

In the early summer of both years, the higher NO_3^- concentrations followed by a progressive decline during the first days, before the occurrence of rain events, likely reflected the nitrate regression phase following the nitrate pulse (Pellerin et al., 2012; Beaton et al., 2017). Indeed, although the main nitrate pulse was not captured in this study, since it generally occurs during the early snow-melt period (e.g., Sebestyen et al., 2008; Pellerin et al., 2012), the depleted isotope values in the pond water and low water temperature suggested a contribution from snow melt (cf., Hayashi, 2020; Marchina et al., 2020; Bearzot et al., 2023). Several studies have shown that the nitrate (and other solute) peak, often observed in montane surface waters during the early phases of snow melt (Johannessen and Henriksen, 1978), originates from the preferential elution of nitrate from the snowpack during the early melting phase (atmospheric origin, Sebestyen et al., 2008),

365 and/or from the flushing of nitrate, produced by microbial nitrification, from catchment soils
366 (terrestrial origin, Campbell et al., 2002; Sickman et al., 2003).

367 In 2014, 5 main rain-on-snow events occurred during the late snow-melt phase, contributing to
368 54 % of the cumulated rain during the entire 2014 monitoring period. During the first event (ca. 40
369 mm), NO_3^- concentrations doubled in 33 hours (from 5.6 to 11.2 µmol L^{-1}) while, for instance, the
370 concentration increase after the third event (ca. 50 mm) was rather reduced (from 8 to 10 µmol L^{-1}).
371 These variations likely reflect the occurrence of new sources of N made available by an increase in
372 the wetness during rain events. Indeed, these events could have increased the fraction of the
373 catchment hydrologically connected to the pond through shallow subsurface and overland flows. At
374 the end of July, an enrichment in the isotopic values of pond water with respect to the preceding
375 days (from −14.8 to −13.6 ‰ for $\delta^{18}O$ and from −106.9 to −96.3 ‰ for $\delta^{2}H$) seems to indicate a
376 relevant hydrological contribution from rain water. Enhanced infiltration could also have favoured
377 the rising of groundwater and saturation of soil, resulting in the release of nitrate originated by
378 nitrification. In addition, NO_3^- could also have derived from the flushing of other debris deposits in
379 the catchment, such as talus, where it could be released by microbial pools (Sickman et al., 2003;
380 Ley et al., 2004; Nemergut et al., 2005). The expansion of the hydrological network, enhancing the
381 interaction between water and soil/debris deposits, might also explain the increase in turbidity, due
382 to the transport of suspended particles to the pond.

383 In 2015, the snow-melt phase lasted few days (29 June – 9 July) however, in this period,
384 pronounced NO_3^- diel cycles (amplitude up to 4.1 µmol L^{-1}) might indicate a connection to the diel
385 variations of the hydrological fluxes originated from snow melt in the catchment. Indeed, previous
386 research using in-situ high-frequency sensors in alpine streams (Pellerin et al., 2012) and proglacial
387 meltwater rivers (Beaton et al., 2017) reported a diurnal nitrate variability caused by variations in
388 diurnal discharge (inverse relationship), during the early and middle stage of the snow melt phase.
389 However, it is not clear why these diel cycles were larger in 2015 with respect to 2014. An

390 explanation might be related to the warmer atmospheric conditions during the snow-melt period in
391 2015, which caused a higher daily snow melt (ca. 6.5 cm day^{-1}) with respect to the one in 2014 (ca.
392 4.5 cm day^{-1}), resulting in potentially larger daily snowmelt fluxes. Unfortunately, the lack of
393 continuous measurements of the pond water level does not allow us to deepen the analysis on this
394 process.
395
396 **4.2 Mid-summer: snow-free season**
397 In 2014, after the July peaks, a decline in NO_3^- concentrations was observed until reaching the
398 minimum values at the end of August (ca. 3 µmol L^{-1}). Concurrently with the NO_3^- decline, a
399 gradual increase in water temperature was measured. The significant negative correlation between
400 water temperature and NO_3^- in 2014 suggests that the biological processes consuming N (e.g., plant
401 uptake and microbial immobilisation), that take place in the pond and in the catchment, played a
402 fundamental role in the nitrate dynamics. A number of studies reported summer relative low values
403 of NO_3^- in alpine forest streams, highlighting the importance of soil biological community in the
404 retention and loss of N and therefore the strict connection between soil and waters in mountain
405 ecosystems (e.g., Balestrini et al., 2006; Helliwell et al., 2007; Curtis et al., 2011). In agreement
406 with these findings, Balestrini et al. (2013) showed a strong positive relation between the areal
407 extension of developed soils and the retention of N in running waters over the treeline.
408 A growing number of studies (e.g., Roberts et al., 2007; Pellerin et al., 2012; Beaton et al., 2017)
409 have shown that in-stream and in-lake processes can also be important drivers of water nutrient
410 concentrations. For instance, Pellerin et al. (2012) and Beaton et al. (2017) attributed the nitrate diel
411 cycles (amplitude 1–2 µmol L^{-1}), detected in a forest stream and in a proglacial lake, to the
412 biological uptake directly linked to autotrophic production. Photosynthesis provides supplementary
413 energy that can be used by biological communities to lessen nitrate for use in metabolism and
414 biosynthesis (Roberts et al., 2007). In lentic systems like ponds, the biological processes occurring

415 within the water column and in the sediments should be even more important compared to lotic
416 waters. In addition, the lack of tree shading and the high radiation intensity should be able to
417 enhance the photosynthesis in aquatic ecosystems over the treeline. The fact that in our case evident
418 nitrate diel cycles were not recorded might be attributable to the low sensitivity of the probe at very
419 low concentrations, which did not allow us to detect NO_3^- variations like those expected as result of
420 autotrophic assimilation. Although the pond lacks the most evident examples of benthic primary
421 producers (e.g., submerged macrophytes and macroalgae), the findings of Mania et al. (2019, 2021)
422 demonstrated the presence of higher proportions of cyanobacterial sequences in the deepest area of
423 the pond and attested that photo- and chemolithoautotrophic bacteria may represent an important
424 component of the total benthic microbial community. Finally, during the entire mid-summer period,
425 rainfall events (cumulated rain: 110 mm) did not strongly affect turbidity (and NO_3^-
426 concentrations), which remained low and stable, possibly indicating a poor hydrological connection
427 between the catchment and the pond. Thus, it is possible to hypothesise that bacterial processes in
428 the pond played a major role in driving the nitrate temporal evolution during the snow-free season,
429 despite a water temperature lower than +11 °C. Another process potentially responsible for the
430 NO_3^- removal is denitrification in pond sediments. However, the quantification of ambient
431 denitrification rate is critical and a relevant gap of knowledge exists concerning this process in
432 small oligotrophic lakes/ponds with very low N concentrations (Seitzinger et al., 2006). Some
433 studies performed in cold and oligotrophic environments (Myrstener et al., 2016; Vila-Costa et al.,
434 2016; Palacin-Lizarbe et al., 2018) reported denitrification rates falling in the low range of
435 freshwater sediments (Seitzinger, 1988; Piña-Ochoa and Alvarez-Cobelas, 2006)

436 The snow-free season 2015 started one month earlier with respect to the 2014's one. During the
437 first two weeks of July, the water temperature increased rapidly (up to ca. +13 °C), while NO_3^-
438 concentrations reached their minimum values (ca. 3 µmol L^{-1}) approximately a month and a half
439 earlier compared to the previous year. The first rain event, after several consecutive dry days,

resulted in a higher and faster NO_3^- (15 µmol L^{-1}) and turbidity (29.7 FTU) peak with respect to the one recorded in July 2014. The rapid decline of both parameters in the following days, when the water temperature was relatively stable, could be attributed to the exhaustion of the N source, such as the organic soils (Schlesinger, 1997; Campbell et al., 2002; Burns et al., 2019) located around the pond (Colombo et al., 2020).

The NO_3^- temporal evolution after the probe malfunction (31 July) was investigated by considering the weekly grab samples. In particular, one more NO_3^- peak (14 µmol L^{-1}) was measured on 13 August, after a heavy rain event that occurred between 8 and 10 August (cumulated rain: 115 mm). The higher soil temperatures measured in 2015 close to the pond (Freppaz et al., 2019) might have enhanced the microbial activity and therefore the mineralisation of organic matter and nitrification (Rogora et al., 2008; Dawes et al., 2017; Donhauser et al., 2021), favouring the release of nitrate during the precipitation events. Enhanced mobilisation due to stronger evapoconcentration in the soil under previous drier conditions might have also played a role (Knapp et al., 2020). Moreover, in addition to the meteorological conditions during the summer season, also the previous snow-covered season might have contributed in influencing the nutrient dynamics in soil and surface water in the area (Freppaz et al., 2019). Specifically, Magnani et al. (2017) demonstrated that a short snow-cover duration, like the one recorded in 2015, may increase soil temperature and substrate availability during the subsequent growing season, favouring soil microbial biomass.

Other processes might have contributed in supplying NO_3^- to the pond during and after the rainfall events, although they were considered of minor importance. For instance, Colombo et al. (2018b, 2019a) showed the role of rainfall in enhancing the export of NO_3^- from the rock glacier. However, the authors also estimated that the hydrochemical influence of the rock glacier on the overall pond was limited in frequency and magnitude, and it was not likely to affect the entire pond in terms of hydrology and water chemistry. The contribution of a direct atmospheric input of NO_3^-

to the pond water cannot be excluded neither. However, taking the mid-August 2015 event as an example, the NO_3^- peak concentration in pond water (14 µmol L^{-1}) was above the mean NO_3^- concentration measured in rain in the area (10 µmol L^{-1}) and during the rain event itself (12.7 µmol L^{-1}), as reported by Colombo et al. (2019a). In addition, previous studies in this area have shown that physical and chemical processes occurring in the catchments, rather than direct precipitation contributions, are likely the predominant drivers in determining nitrate concentrations, and their seasonal variations, in surface waters (Magnani et al., 2017; Colombo et al., 2019a,b; Freppaz et al., 2019).

4.3 Late summer-fall transition

The behaviour of NO_3^- during September and October 2014 was the opposite of that observed in the previous two months. Indeed, increasing NO_3^- concentrations, in conjunction with decreasing water temperatures, were observed. Some rain events interrupted the gradual evolution of both parameters with sharper changes depending on rainfall intensity and duration. Turbidity also showed a response to the latest rain events, although its response occurred later and was weaker compared to the one of NO_3^-. The available weekly data exhibited a similar NO_3^- pattern in 2015. Indeed, the NO_3^- concentration increased from 3.7 µmol L^{-1}, at the beginning of September, to 6.4 µmol L^{-1}, after a month. The NO_3^- concentration at the end of the season was comparable to that recorded in 2014, suggesting a sort of stability in the processes characterising this aquatic ecosystem. This nitrate behaviour during the late summer-fall transition phase is coherent with the findings of Freppaz et al. (2019) in a nearby pond, and with similar reports from alpine tundra (Sickman at al., 2003; Balestrini et al., 2013; Williams et al., 2015a) and alpine forest areas (Balestrini et al., 2006; Rusjan and Mikos, 2010). The common hypothesis explaining the increase in nitrate is the slowdown of the biologically-mediated immobilisation processes in soil, due to colder soil temperature at the end of summer. In these conditions, the possible transfer of nitrate to

the pond depends on rainfall occurrence. In addition, the temperature decrease can affect the in-pond nutrient uptake (cf., Roberts et al., 2007), also lowering the photosynthetic activity. Consequently, the autotrophic community might play a role in N retention during this season (Rusjan and Mikos, 2010; Oleksy et al., 2021).

Nitrate increase due to simple concentration as a result of evaporation might be also considered. However, in this phase of the season, the increases of NO_3^- were observed during colder atmospheric periods. In addition, the distribution of the stable water isotopic data was consistent with the NIMWL. Thus, results suggest that evaporation can be considered a negligible process in isotope fractionation in the pond, since it would have caused an enrichment in $\delta^{18}O$ and a subsequent decrease in the distribution slope with respect to the NIMWL. It is also true that, in both years, the water level of the pond, measured on a weekly basis by Colombo et al. (2018a), progressively decreased from June/July to October, thus this might seem to point towards a role of evaporation, considering the lack of stable pond outflows. However, this water level decrease was found to be mostly driven by a sub-surface seepage at the pond bottom, where a minor fault zone in bedrock is located, characterised by altered and highly-fractured rocks (Colombo et al., 2018a). Finally, isotopically-enriched groundwater (cf., Fan et al. 2022), possibly nitrate-concentrated, might also have provided a higher contribution in late summer-early fall (cf., Hayashi, 2020). Unfortunately, the contribution of groundwater, that was not sampled in this study since no groundwater springs are present in the analysed catchment, is not easy to disentangle when dealing with high-elevation lakes and ponds, especially in the absence of stable surface inflows/outflows (cf., Langston et al., 2013), like in the study site. Thus, the role of groundwater in supplying NO_3^- in this high-elevated setting must be further investigated.

4.4 Environmental implications and research/operative perspectives

514 The complex interplay between rainfall, snow melt, and temperature (water and air) during the
515 summer season showed the capability to drive daily and seasonal NO_3^- concentrations in the
516 investigated pond. In the European Alps, significant increases in air temperature (Gobiet et al.,
517 2014) and snow line elevation (Koehler et al., 2022), as well as reductions in snow cover duration
518 (Klein et al., 2016), snow depth (Matiu et al., 2021), and snow water equivalent (Marty et al., 2017;
519 Colombo et al., 2022; 2023), have occurred in the last decades. These occurrences are expected to
520 become even more dramatic in the future (Gobiet et al., 2014; Beniston et al., 2018). Regional
521 climate model simulations also indicate that summer rainfall at Alpine high elevations will increase
522 due to global warming, despite the expected large-scale precipitation reduction (Giorgi et al., 2016)
523 and drought event increases (Spinoni et al., 2018), together with potential increases in heavy
524 precipitation and hot temperature extremes (Scherrer et al., 2016). Furthermore, rain-on-snow
525 events are also predicted to increase in the next decades (Beniston and Stoffel, 2016).
526 The alteration of the hydrological cycle induced by climate change (e.g., changes in runoff peak
527 and timing together with modifications in the water residence time) could have a great influence on
528 both N input and removal to/from aquatic ecosystems (e.g., Baron et al., 2013). In addition, during
529 dry periods, leaching of NO_3^- from soils is reduced/absent due to low hydraulic conductivity in the
530 soil profile. As a consequence, the residence time of potentially leachable N in soils (and its plant
531 uptake) as well as microbial immobilisation could increase. Then, this N temporally stored in soils
532 could be mobilised (NO_3^-) / mineralised (organic N) and leached in the following wet periods. In
533 the present study, the N dynamics were analysed and compared in two years characterised by
534 extremely different meteoclimatic conditions and features that might be typical under the climate
535 change impacts, such as very high air temperature, heavy rainfalls, and rain-on-snow events. In
536 2015, a higher N supply to the pond was found, in the form of peaks due to rapid and intense
537 hydrological flows. These events occurred in the mid-summer phase when the biological N uptake
538 is commonly maximum and thus minimal NO_3^- values are expected. This is even more evident if

compared to the NO_3^- dynamics in 2014, when the relatively stable meteoclimatic conditions during mid-summer led to limited variations and low concentrations of NO_3^-. Moreover, this study further highlights the role of air and water temperature in controlling the N production and retention at daily and seasonal time scale. In the snow-free season, when dry conditions occur and the pond is therefore hydrologically disconnected from the catchment, water temperature could be used as a robust predictor of pond water NO_3^- concentration. Only by using an approach based on in-situ high-frequency measurements it was possible to fully grasp both the effect of hydrological processes and the role of in-lake nutrient biological retention processes in the N dynamics in the Col d'Olen Rock Glacier Pond, representative of ultraoligotrophic water bodies in alpine tundra. Finally, the high-resolution temporal assessment of nitrate dynamics could also avoid potentially misleading comparisons of water chemistry collected through synoptic surveys during different seasons and years, and improve the understanding of the connections between surface water, soil water and groundwater in these remote environments.

Future work could take into consideration the use of longer measuring path lengths to increase the accuracy and sensitivity of the UV–Vis probe at these low concentrations, which are at the lower end of the probe measurement range. In addition, performing local calibrations using samples taken from the actual water investigated will help account for the matrix effect and thus further increase the measurement accuracy. In this context, a consistent number of samples (for instance, 40–50, half for calibration and half for validation) could be collected in order to improve the probe performance assessment, also taking into account a possible wider range of nitrate concentrations. However, considering a weekly sampling plan and the fact that ponds like the one analysed in this study are typically ice-free for a limited amount of time (maximum 3/4 months), the collection of a large number of samples would require the in-situ maintenance of the probe for three or more ice-free seasons, which could be hard to perform is such highly elevated remote areas. Thus, alternatively, a focus on shorter periods could be recommended, such as during the snow-ionic

pulse (if the ice conditions on the pond will allow the installation of the probe), late snow melt, in-lake retention conditions during period with poor hydrological connection, or single months for the monitoring of possible heavy rain events; in turn, a larger number of samples could be collected, even on a daily basis. Finally, performing measurements with a greater sensitivity is considered necessary to properly investigate the diel variability of nitrate in order to verify the occurrence of a retention process strictly connected to the photosynthesis (e.g., autotrophic assimilation). In this regard, the high-frequency measurement of O_2 to explore the extent of diel variations and to record the groundwater inflow would be beneficial for supporting the interpretation of the NO_3^- analysis.

5 Conclusions

This study reports on the first use of a UV–Vis submersible spectrophotometric probe in association with weekly analyses of NO_3^--N and stable isotopes of water ($\delta^{18}O$ and $\delta^{2}H$), together with continuous meteorological, water temperature and turbidity measurements, in a high-elevation pond in alpine tundra. The proposed approach allowed disentangling the complex effects, and their interplay, of snow melt, temperature (air and water), and summer rainfall on nitrate dynamics. In particular, snow-melt duration and temperature fluctuations drove the nitrate variations on a seasonal basis, also determining the timing of the seasonal transitions. However, short-duration meteorological events (lasting even few hours), such as heavy rainfalls and rain-on-snow events, deeply disrupted these dynamics, in the form of NO_3^- peaks due to rapid and intense hydrological flows, which lasted up to few days/weeks. The effects of these hydrological events were properly assessed thanks to the use of in-situ high-frequency measurements, which also allowed to better define the role of in-lake nutrient biological retention processes in the N dynamics in the investigated ultraoligotrophic pond. Therefore, high-resolution temporal monitoring of nitrate dynamics may contribute to a better understanding of the biogeochemical processes occurring in these remote, yet highly sensitive environments. Ultimately, this could help predicting how the

quality of high-elevation surface waters will respond to changing climate and related climate extremes (e.g., reduction in snow-cover duration and increases in magnitude and frequency of heavy rainfall events).

Acknowledgments

We thank Elena Serra, Elisa Giaccone, Andrea Magnani, Diego Guenzi, Maria Chiara Caschetto, and Davide Viglietti for their help in fieldwork and laboratory activities. We give special thanks to Mark Williams and Holly Hughes (Department of Geography, University of Colorado, Boulder, USA), Consorzio di Miglioramento Fondiario di Gressoney (Aosta), Monterosa Spa and Monterosa 2000 (Monterosa ski). This research was supported by the PRIN 2010-11 (funded project of the Italian Ministry for Education and Research) named "Response of morphoclimatic system dynamics to global changes and related geomorphological hazards" (coord. Prof. Carlo Baroni). Nicola Colombo and Michele Freppaz were partially supported by the project NODES, which has received funding from the MUR–M4C2 1.5 of PNRR with grant agreement no. ECS00000036. We would like to dedicate this paper to the memory of our colleague Simona Fratianni, who passed away prematurely.

Conflict of interest

The authors declare there are no competing interests.

Contributions

Conceptualisation: NC and FS. Investigation: NC, DG, GV, and FS. Methodology and Formal analysis: NC, DG, RB, and FS. Data curation, Software, and Visualisation: DG and NC. Funding acquisition: FS, MF, and SF. Writing - original draft: NC and RB. Writing - review & editing: all authors.

615 **References**

616 Aber J, McDowell W, Nadelhoffer K, Magill A, Berntson G, Kamakea M, McNulty S, Currie W,
617 Rustad L, Fernandez I, 1998. Nitrogen Saturation in Temperate Forest Ecosystems: Hypotheses
618 revisited. BioScience 48(11):921–934. https://doi.org/10.2307/1313296

619 Adrian R, O'Reilly CM, Zagarese H, Baines SB, Hessen DO, Keller W, Livingstone DM,
620 Sommaruga R, Straile D, Van Donk E, Weyhenmeyer GA, Winder M, 2009. Lakes as sentinels
621 of climate change. Limnol. Oceanogr. 54(6):2283–2297.
622 https://doi.org/10.4319/lo.2009.54.6_part_2.2283

623 Balestrini R, Di Martino N, Van Miegroet H, 2006. Nitrogen cycling and mass balance for a
624 forested catchment in the Italian Alps. Biogeochemistry 78:97–123.
625 https://doi.org/10.1007/s10533-005-3429-7

626 Balestrini R, Arese C, Freppaz M, Buffagni A, 2013. Catchment features controlling nitrogen
627 dynamics in running waters above the tree line (central Italian Alps). Hydrol. Earth Syst. Sci.
628 17(3):989–1001. https://doi.org/10.5194/hess-17-989-2013

629 Barnes RT, Williams MW, Parman JN, Hill K, Caine N, 2014. Thawing glacial and permafrost
630 features contribute to nitrogen export from Green Lakes Valley, Colorado Front Range, USA.
631 Biogeochemistry 117:413–430. https://doi.org/10.1007/s10533-013-9886-5

632 Baron JS., Hall EK, Nolan BT, Finlay JC, Bernhardt ES, Harrison JA, Chan F, Boyer EW, 2013.
633 The interactive effects of excess reactive nitrogen and climate change on aquatic ecosystems and
634 water resources of the United States. Biogeochemistry 114:71–92.
635 https://doi.org/10.1007/s10533-012-9788-y

636 Bearzot F, Colombo N, Cremonese E, Morra di Cella U, Drigo E, Caschetto M, Basiricò S, Crosta
637 GB, Frattini P, Freppaz M, Pogliotti P, Salerno F, Brunier A, Rossini M, 2023. Hydrological,
638 thermal and chemical influence of an intact rock glacier discharge on mountain stream water.
639 Sci. Total Environ. 876:162777. https://doi.org/10.1016/j.scitotenv.2023.162777

Beaton AD, Wadham JL, Hawkings J, Bagshaw EA, Lamarche-Gagnon G, Mowlem MC, Tranter M, 2017. High-Resolution in situ measurement of nitrate in runoff from the Greenland Ice Sheet. Environ. Sci. Technol. 51(21):12518–12527. https://doi.org/10.1021/acs.est.7b03121

Beniston M, Stoffel M, 2016. Rain-on-snow events, floods and climate change in the Alps: Events may increase with warming up to 4 °C and decrease thereafter. Sci. Total Environ. 571:228–236. https://doi.org/10.1016/j.scitotenv.2016.07.146

Beniston M, Farinotti D, Stoffel M, Andreassen LM, Coppola E, Eckert N, Fantini A, Giacona F, Hauck C, Huss M, Huwald H, Lehning M, López-Moreno J-I, Magnusson J, Marty C, Morán-Tejéda E, Morin S, Naaim M, Provenzale A, Rabatel A, Six D, Stötter J, Strasser U, Terzago S, Vincent C, 2018. The European mountain cryosphere: a review of its current state, trends, and future challenges. Cryosphere 12:759–794. https://doi.org/10.5194/tc-12-759-2018

Brighenti S, Engel M, Tolotti M, Bruno MC, Wharton G, Comiti F, Tirler W, Cerasino L, Bertoldi W, 2021. Contrasting physical and chemical conditions of two rock glacier springs. Hydrol. Process. 35:e14159. https://doi.org/10.1002/hyp.14159

Burns DA, Pellerin BA, Miller MP, Capel PD, Tesorieri AJ, Duncan JM, 2019. Monitoring the riverine pulse: Applying high-frequency nitrate data to advance integrative understanding of biogeochemical and hydrological processes. WIREs Water 6(4):e1348. https://doi.org/10.1002/wat2.1348

Campbell DH, Kendall C, Chang CCY, Silva SR, Tonnessen KA, 2002. Pathways for nitrate release from an alpine watershed: Determination using $\delta^{15}N$ and $\delta^{18}O$. Water Resour. Res. 38(5):10-1–10-9. https://doi.org/10.1029/2001WR000294

Carvalho L, 2015. An improved evaluation of Kolmogorov's distribution. J. Stat. Softw. 65:1–8. doi: 10.18637/jss.v065.c03

Catalan J, Camarero L, Felip M, Pla S, Ventura M, Buchaca T, Bartumeus F, De Mendoza G, Miró A, Casamayor EO, Medina-Sánchez JM, Bacardit M, Altuna M, Bartrons M, Díaz De Quijano

665 D, 2006. High mountain lakes: Extreme habitats and witnesses of environmental changes.
666 Limnetica 25(1-2):551–584. DOI:10.23818/limn.25.38
667 Clow DW, Sickman JO, Striegl RG, Krabbenhoft DP, Elliott JG, Dornblaser M, Roth DA,
668 Campbell DH, 2003. Changes in the chemistry of lakes and precipitation in high-elevation
669 national parks in the western United States, 1985–1999. Water Resour. Res. 39(6):1171–1184.
670 https://doi.org/10.1029/2002WR001533
671 Colombo N, Sambuelli L, Comina C, Colombero C, Giardino M, Gruber S, Viviano G, Vittori
672 Antisari L, Salerno F, 2018a. Mechanisms linking active rock glaciers and impounded surface
673 water formation in high-mountain areas. Earth Surf. Process. Landf. 43(2):417–431.
674 https://doi.org/10.1002/esp.4257
675 Colombo N, Gruber S, Martin M, Malandrino M, Magnani A, Godone D, Freppaz M, Fratianni S,
676 Salerno F, 2018b. Rainfall as primary driver of discharge and solute export from rock glaciers:
677 the Col d'Olen Rock Glacier in the NW Italian Alps. Sci. Total Environ. 639:316–330.
678 https://doi.org/10.1016/j.scitotenv.2018.05.098
679 Colombo N, Salerno F, Martin M, Malandrino M, Giardino M, Serra E, Godone D, Said-Pullicino
680 D, Fratianni S, Paro L, Tartari G, Freppaz M, 2019a. Influence of permafrost, rock and ice
681 glaciers on chemistry of high-elevation ponds (NW Italian Alps). Sci. Total Environ. 685:886–
682 901. https://doi.org/10.1016/j.scitotenv.2019.06.233
683 Colombo N, Bocchiola D, Martin M, Confortola G, Salerno F, Godone D, D'Amico ME, Freppaz
684 M, 2019b. High export of nitrogen and dissolved organic carbon from an Alpine glacier (Indren
685 Glacier, NW Italian Alps). Aquat. Sci. 81:74. doi.org/10.1007/s00027-019-0670-z
686 Colombo N, Ferronato C, Vittori Antisari L, Marziali L, Salerno F, Fratianni S, D'Amico ME,
687 Ribolini A, Godone D, Sartini S, Paro L, Morra di Cella U, Freppaz M, 2020. A rock-glacier–
688 pond system (NW Italian Alps): Soil and sediment properties, geochemistry, and trace-metal
689 bioavailability. Catena 194:104700. https://doi.org/10.1016/j.catena.2020.104700

690 Colombo N, Valt M, Romano E, Salerno F, Godone D, Cianfarra P, Freppaz M, Maugeri M,
691 Guyennon N, 2022. Long-term trend of snow water equivalent in the Italian Alps. J. Hydrol.
692 614(A). https://doi.org/10.1016/j.jhydrol.2022.128532
693 Colombo N, Guyennon N, Valt M, Salerno F, Godone D, Cianfarra P, Freppaz M, Maugeri M,
694 Manara V, Acquaotta F, Pietrangeli AB, Romano E, 2023. Unprecedented snow-drought
695 conditions in the Italian Alps during the early 2020s. Environ. Res. Lett. 18:074014.
696 https://doi.org/10.1088/1748-9326/acdb88
697 Curtis C, Evans C, Goodale C, Heaton T., 2011. What have stable isotope studies revealed about the
698 nature and mechanisms of N Saturation and nitrate leaching from semi-natural catchments?,
699 Ecosystems 14:1021–1037. https://www.jstor.org/stable/41505929
700 Dawes MA, Schleppi P, Hättenschwiler S, Rixen C, Hagedorn F, 2017. Soil warming opens the
701 nitrogen cycle at the alpine treeline. Glob. Chang. Biol. 23(1):421–434.
702 https://doi.org/10.1111/gcb.13365
703 Donhauser J, Qi W, Bergk-Pinto B, Frey B, 2021. High temperatures enhance the microbial genetic
704 potential to recycle C and N from necromass in high-mountain soils. Glob. Chang. Biol.
705 27(7):1365–1386. https://doi.org/10.1111/gcb.15492
706 Edwards AC, Hooda PS, Cook Y, 2001. Determination of nitrate in water containing dissolved
707 organic carbon by ultraviolet spectroscopy. Int. J. Environ. Anal. Chem. 80(I):49–59.
708 https://doi.org/10.1080/03067310108044385
709 Elser JJ, Kyle M, Steger L, Nydick KR, Baron JS, 2009. Nutrient availability and phytoplankton
710 nutrient limitation across a gradient of atmospheric nitrogen deposition. Ecology 90(11):3062–
711 3073. https://doi.org/10.1890/08-1742.1
712 Fan Y, Wu Y, Wang Y, Jiang S, Yu S, Shang H, 2022. An Analysis of Surface Water–
713 Groundwater Interactions Based on Isotopic Data from the Kaidu River Basin, South Tianshan
714 Mountain. Water 14:2259. https://doi.org/10.3390/w14142259

715 Fleischmann N, Langergraber G, Weingartner A, Hofstaedter F, Nusch S, Maurer P, 2001. On-line
716 and in-situ measurement of turbidity and COD in wastewater using UV/VIS spectrometry.
717 SCAN Media Library. https://www.s-can.at/wp_contents/uploads/2021/09/p_2001_06.pdf
718 Freppaz M, Viglietti D, Balestrini R, Lonati M, Colombo N, 2019. Climatic and pedoclimatic
719 factors driving C and N dynamics in soil and surface water in the alpine tundra (NW-Italian
720 Alps). Nat. Conserv. 34:67–90. https://doi.org/10.3897/natureconservation.34.30737
721 Giorgi F, Torma C, Coppola E, Ban N, Schär C, Somot S, 2016. Enhanced summer convective
722 rainfall at alpine high elevations in response to climate warming. Nat. Geosci. 9:584–589.
723 https://doi.org/10.1038/ngeo2761
724 Gobiet A, Kotlarski S, Beniston M, Heinrich G, Rajczak J, Stoffel M, 2014. 21st century climate
725 change in the European Alps: a review. Sci. Total Environ. 493:1138–1151.
726 https://doi.org/10.1016/j.scitotenv.2013.07.050
727 Hamerlík L, Svitok M, Novikmec M, Očadlík M, Bitušík P, 2014. Local, among-site, and regional
728 diversity patterns of benthic macroinvertebrates in high altitude waterbodies: Do ponds differ
729 from lakes? Hydrobiologia 723(1):41–52. https://doi.org/10.1007/s10750-013-1621-7
730 Hayashi M, 2020. Alpine hydrogeology: The critical role of groundwater in sourcing the
731 headwaters of the world. Groundwater 58:498–510. https://doi.org/10.1111/gwat.12965
732 Helliwell RC, Coull MC, Davies JJL, Evans CD, Norris D, Ferrier RC, Jenkins A, Reynolds B,
733 2007. The role of catchment characteristics in determining surface water nitrogen in four upland
734 regions in the UK. Hydrol. Earth Syst. Sci. 11(1):356–371, https://doi.org/10.5194/hess-11-356-
735 2007
736 Huebsch M, Grimmeisen F, Zemann M, Fenton O, Richards KG, Jordan P, Sawarieh A, Blum P,
737 Goldscheider N, 2015. Technical Note: Field experiences using UV/VIS sensors for high-
738 resolution monitoring of nitrate in groundwater. Hydrol. Earth Syst. Sci. 19:1589–1598.
739 https://doi.org/10.5194/hess-19-1589-2015

740 Johannessen M, Henriksen A, 1978. Chemistry of snow meltwater: Changes in concentration during
741 melting. Water Resour. Res. 14(4):615–619. https://doi.org/10.1029/WR014i004p00615
742 Klein G, Vitasse Y, Rixen C, Marty C, Rebetez M, 2016. Shorter snow cover duration since 1970 in
743 the Swiss alps due to earlier snowmelt more than to later snow onset. Clim. Chang. 139(3):637–
744 649. https://doi.org/10.1007/s10584-016-1806-y
745 Knapp JLA, Freyberg J, Studer B, Kiewiet L, Kirchner JW, 2020. Concentration–discharge
746 relationships vary among hydrological events, reflecting differences in event characteristics.
747 Hydrol. Earth Syst. Sci. 24:2561–2576. https://doi.org/10.5194/hess-24-2561-2020
748 Koehler J, Bauer A, Dietz AJ, Kuenzer C, 2022. Towards Forecasting Future Snow Cover
749 Dynamics in the European Alps—The Potential of Long Optical Remote-Sensing Time Series.
750 Remote Sens. 14:4461. https://doi.org/10.3390/rs14184461
751 Kopáček J, Stuchlík E, Wright RF, 2005. Long-term trends and spatial variability in nitrate leaching
752 from alpine catchment–lake ecosystems in the Tatra Mountains (Slovakia–Poland). Environ.
753 Pollut. 135(1):89–101. https://doi.org/10.1016/j.envpol.2004.12.012
754 Langergraber G, Fleischmann N, Hofstädter F, 2003. A multivariate calibration procedure for
755 UV/VIS spectrometric quantification of organic matter and nitrate in wastewater. Water Sci.
756 Technol. 47:63–71. https://doi.org/10.2166/wst.2003.0086
757 Langston G, Hayashi M, Roy JW, 2013. Quantifying groundwater-surface water interactions in a
758 proglacial moraine using heat and solute tracers. Water Resour. Res. 49(9):5411–5426.
759 https://doi.org/10.1002/wrcr.20372
760 Ley RE, Williams MW, Schmidt SK, 2004. Microbial population dynamics in an extreme
761 environment: Controlling factors in talus soils at 3750 m in the Colorado Rocky Mountains.
762 Biogeochemistry 68:297–311. https://doi.org/10.1023/B:BIOG.0000031032.58611.d0
763 Longinelli A, Selmo E, 2003. Isotopic composition of precipitation in Italy: a first overall map. J.
764 Hydrol. 270:75–88. https://doi.org/10.1016/S0022-1694(02)00281-0

ha formattato: Inglese (Regno Unito)

765 Magnani A, Viglietti D, Balestrini R, Williams MW, Freppaz M, 2017. Contribution of deeper soil
766 horizons to N and C cycling during the snow-free season in alpine tundra, NW Italy. Catena
767 155:75–85. https://doi.org/10.1016/j.catena.2017.03.007
768 Mania I, Gorra R, Colombo N, Freppaz M, Martin M, Anesio AM, 2019. Prokaryotic diversity and
769 distribution in different habitats of an alpine rock glacier-pond system. Microb. Ecol. 78(1):70–
770 84. https://doi.org/10.1007/s00248-018-1272-3
771 Mania I, Pellicciaro M, Gorra R, 2021. Insights into the microbial autotrophic potential of a shallow
772 oligotrophic alpine pond. Mar. Freshw. Res. 72(6):899–903. https://doi.org/10.1071/MF20241
773 Marchina C, Lencioni V, Paoli F, Rizzo M, Bianchini G, 2020. Headwaters' Isotopic Signature as a
774 Tracer of Stream Origins and Climatic Anomalies: Evidence from the Italian Alps in Summer
775 2018. Water 12(2):390. https://doi.org/10.3390/w12020390
776 Marty C, Tilg A-M, Jonas T, 2017. Recent evidence of large scale receding snow water equivalents
777 in the European Alps. J. Hydrometeorol. 18:1021–1031. https://doi.org/10.1175/JHM-D-16-
778 0188.1
779 Matiu M, Crespi A, Bertoldi G, Carmagnola CM, Marty C, Morin S, Schöner W, Cat Berro D,
780 Chiogna G, De Gregorio L, Kotlarski S, Majone B, Resch G, Terzago S, Valt M, Beozzo W,
781 Cianfarra P, Gouttevin I, Marcolini G, Notarnicola C, Petitta M, Scherrer SC, Strasser U,
782 Winkler M, Zebisch M, Cicogna A, Cremonini R, Debernardi A, Faletto M, Gaddo M,
783 Giovannini L, Mercalli L, Soubeyroux J-M, Sušnik A, Trenti A, Urbani S, Weilguni V, 2021.
784 Observed snow depth trends in the European Alps: 1971 to 2019. Cryosphere 15:1343–1382.
785 https://doi.org/10.5194/tc-15-1343-2021
786 Mladenov N, Lípez-Ramos J, McKnight DM, Rechea I, 2009. Alpine lake optical properties as
787 sentinels of dust deposition and global change. Limnol. Oceanogr. 54:2386–2400.
788 https://doi.org/10.4319/lo.2009.54.6_part_2.2386

Mulholland PJ, Thomas SA, Valett HM, Webster JR, Beaulieu J, 2006. Effects of light on NO_3^- uptake in small forested streams: diurnal and day-to-day variations. J. N. Am. Benthol. Soc. 25:583–595. https://doi.org/10.1899/0887-3593(2006)25[583:EOLONU]2.0.CO;2

Myrstener M, Jonsson A, Bergstrom AK, 2016. The effects of temperature and resource availability on denitrification and relative N_2O production in boreal lake sediments. J. Environ. Sci. 47:82–90. https://doi.org/10.1016/j.jes.2016.03.003

Nemergut DR, Costello EK, Meyer AF, Pescador MY, Weintraub MN, Schmidt SK, 2005. Structure and function of alpine and arctic soil microbial communities. Res. Microbiol. 156:775–784. https://doi.org/10.1016/j.resmic.2005.03.004

Oleksy IA, Baron JS, Beck WS, 2021. Nutrients and warming alter mountain lake benthic algal structure and function. Freshw. Sci. 40(1):88–102. https://doi.org/10.1086/713068

Palacin-Lizarbe C, Camarero L, Catalan J, 2018. Denitrification temperature dependence in remote, cold, and N-poor lake sediments. Water Resour. Res. 54:1161–1173. https://doi.org/10.1002/2017WR021680

Pellerin BA, Saraceno JF, Shanley JB, Sebestyen SD, Aiken GR, Wollheim WM, Bergamaschi BA, 2012. Taking the pulse of snowmelt: in situ sensors reveal seasonal, event and diurnal patterns of nitrate and dissolved organic matter variability in an upland forest stream. Biogeochemistry 108:183–198. https://doi.org/10.1007/s10533-011-9589-8

Piña-Ochoa E, Alvarez-Cobelas M, 2006. Denitrification in aquatic environments: A cross-system analysis. Biogeochemistry 81(1):111–130. https://www.jstor.org/stable/20456415

R Core Team, 2022. R: A Language and Environment for Statistical Computing. R Foundation for Statistical Computing, Vienna, Austria URL. https://www.R-project.org/

Roberts BJ, Mulholland PJ, 2007. In-stream biotic control on nutrient biogeochemistry in a forested stream, West Fork of Walker Branch. J. Geophys. Res. Biogeosci. 112:G04002. https://doi.org/10.1029/2007JG000422

ha formattato: Italiano (Italia)

ha formattato: Italiano (Italia)

814 Rusjan S, Mikoš M, 2010. Seasonal variability of diurnal instream nitrate concentration oscillations
815 under hydrologically stable conditions. Biogeochemistry 97:123–140.
816 https://doi.org/10.1007/s10533-009-9361-5
817 Rogora M, Arese C, Balestrini R, Marchetto A, 2008. Climate control on sulphate and nitrate
818 concentrations in alpine streams of Northern Italy along a nitrogen saturation gradient. Hydrol.
819 Earth Syst. Sci. 12(2):371–381. https://doi.org/10.5194/hess-12-371-2008
820 Rogora M, Arisci S, Marchetto A, 2012. The role of nitrogen deposition in the recent nitrate decline
821 in lakes and rivers in Northern Italy. Sci. Total Environ. 417-418:214–223.
822 https://doi.org/10.1016/j.scitotenv.2011.12.067
823 Rogora M, Somaschini L, Marchetto A, Mosello R, Tartari GA, Paro L, 2020. Decadal trends in
824 water chemistry of Alpine lakes in calcareous catchments driven by climate change. Sci. Total
825 Environ. 708:135180. https://doi.org/10.1016/j.scitotenv.2019.135180
826 Salerno F, Thakuri S, Guyennon N, Viviano G, Tartari G, 2016a. Glacier melting and precipitation
827 trends detected by surface area changes in Himalayan ponds. Cryosphere 10(4):1433–1448.
828 https://doi.org/10.5194/tc-10-1433-2016
829 Salerno F, Rogora M, Balestrini R, Lami A, Tartari GA, Thakuri S, Godone D, Freppaz M, Tartari
830 G, 2016b. Glacier melting increases the solute concentrations of Himalayan glacial lakes.
831 Environ. Sci. Technol. 50(17):9150–9160. https://doi.org/10.1021/acs.est.6b02735
832 Sambuelli L, Colombo N, Giardino M, Godone D, 2015. A Waterborne GPR Survey to Estimate
833 Fine Sediments Volume and Find Optimum Core Location in a Rockglacier Lake. Near Surface
834 Geoscience 2015, 21st European Meeting of Environmental and Engineering Geophysics.
835 https://doi.org/10.3997/2214-4609.201413826
836 Scherrer SC, Fischer EM, Posselt R, Liniger MA, Croci-Maspoli M, Knutti R, 2016. Emerging
837 trends in heavy precipitation and hot temperature extremes in Switzerland. J. Geophys. Res.
838 Atmos. 121:2626–2637. https://doi.org/10.1002/2015JD024634

Schlesinger WH, 1997. Biogeochemistry: An Analysis of Global Change. third ed. Academic Press, San Diego.

Sebestyen SD, Boyer EW, Shanley JB, Kendall C, Doctor DH, Aiken GR, Ohte N, 2008. Sources, transformations, and hydrological processes that control stream nitrate and dissolved organic matter concentrations during snowmelt in an upland forest. Water Resour. Res. 44(12). https://doi.org/10.1029/2008WR006983

Seitzinger SP, 1988. Denitrification in fresh-water and coastal marine ecosystems: Ecological and geochemical significance. Limnol. Oceanogr. 33(4):702–724. https://doi.org/10.4319/lo.1988.33.4part2.0702

Seitzinger S, Harrison JA, Böhlke JK, Bouwman AF, Lowrance R, Peterson B, Tobias C, Van Drecht G, 2006. Denitrification across landscapes and waterscapes: a synthesis. Ecol. Appl. 16:2064–2090. https://doi.org/10.1890/1051-0761(2006)016[2064:DALAWA]2.0.CO;2

Slemmons KE, Rodgers ML, Stone JR, Saros JE, 2017. Nitrogen subsidies in glacial meltwaters have altered planktonic diatom communities in lakes of the US Rocky Mountains for at least a century. Hydrobiologia 800(1):129–144. https://doi.org/10.1007/s10750-017-3187-2

Sickman JO, Leydecker A, Chang CCY, Kendall C, Melack JM, Lucero DM, Schimel J, 2003. Mechanisms underlying export of N from high-elevation catchments during seasonal transition. Biogeochemistry 64(1):1–24. https://doi.org/10.1023/A:1024928317057

Snazelle TT, 2015. Results from laboratory and field testing of nitrate measuring spectrophotometers: U.S. Geological Survey Open-File Report 2015–1065, 35 p. http://dx.doi.org/10.3133/ofr20151065

Spinoni J, Vogt JV, Naumann G, Barbosa P, Dosio A, 2018. Will drought events become more frequent and severe in Europe? Int. J. Climatol. 38(4):1718–1736. https://doi.org/10.1002/joc.5291

Tartari G, Salerno F, Buraschi E, Bruccoleri G, Smiraglia C, 2008. Lake surface area variations in the North-Eastern sector of Sagarmatha National Park (Nepal) at the end of the 20th Century by comparison of historical maps. J. Limnol. 67(2):139. https://doi.org/10.4081/jlimnol.2008.139

Tolotti M, Forsström L, Morabito G, Thaler B, Stoyneva M, Cantonati M, Šiško M, Lotter A, 2009. Biogeographical characterisation of phytoplankton assemblages in high altitude, and high latitude European lakes. Adv. Limnol. 62:55–75. https://doi.org/10.1127/advlim/62/2009/55

Vila-Costa M, Pulido C, Chappuis E, Calviño A, Casamayor EO, Gacia E, 2016. Macrophyte landscape modulates lake ecosystem level nitrogen losses through tightly coupled plant-microbe interactions. Limnol. Oceanogr. 61:78–88. https://doi.org/10.1002/lno.10209

Vione D, Colombo N, Said-Pullicino D, Bocchiola D, Confortola G, Salerno F, Viviano G, Fratianni S, Martin M, Godone D, Freppaz M, 2021. Seasonal variations in the optical characteristics of dissolved organic matter in glacial pond water. Sci. Total Environ. 759:143464. https://doi.org/10.1016/j.scitotenv.2020.143464

Viviroli D, Dürr HH, Messerli B, Meybeck M, Weingartner R, 2007. Mountains of the world, water towers for humanity: Typology, mapping, and global significance. Water Resour. Res. 43:1–13. https://doi.org/10.1029/2006WR005653

Viviroli D, Kummu M, Meybeck M, Kallio M, Wada Y, 2020. Increasing dependence of lowland populations on mountain water resources. Nat. Sustain. 3:917–928. https://doi.org/10.1038/s41893-020-0559-9

Williams MW, Losleben MV, Hamann HB, 2002. Alpine areas in the Colorado Front Range as monitors of climate change and ecosystem response. Geogr. Rev. 92(2):180–191. doi:10.2307/4140969

Williams MW, Knauf M, Cory R, Caine N, Liu F, 2007. Nitrate content and potential microbial signature of rock glacier outflow, Colorado Front Range. Earth Surf. Process. Landf. 32:1032–1047. https://doi.org/10.1002/esp.1455

888 Williams MW, Seastedt TR, Bowman WD, McKnight DM, Suding, KN, 2015a. An overview of
889 research from a high elevation landscape: the Niwot Ridge, Colorado long term ecological
890 research programme. Plant Ecol. Divers. 8(5–6):597–605.
891 https://doi.org/10.1080/17550874.2015.1123320
892 Williams MW, Hood E, Molotch NP, Caine N, Cowie R, Liu F, 2015b. The 'teflon basin' myth:
893 hydrology and hydrochemistry of a seasonally snow-covered catchment. Plant Ecol. Divers. 8(5–
894 6):639–661. https://doi.org/10.1080/17550874.2015.1123318

Figures

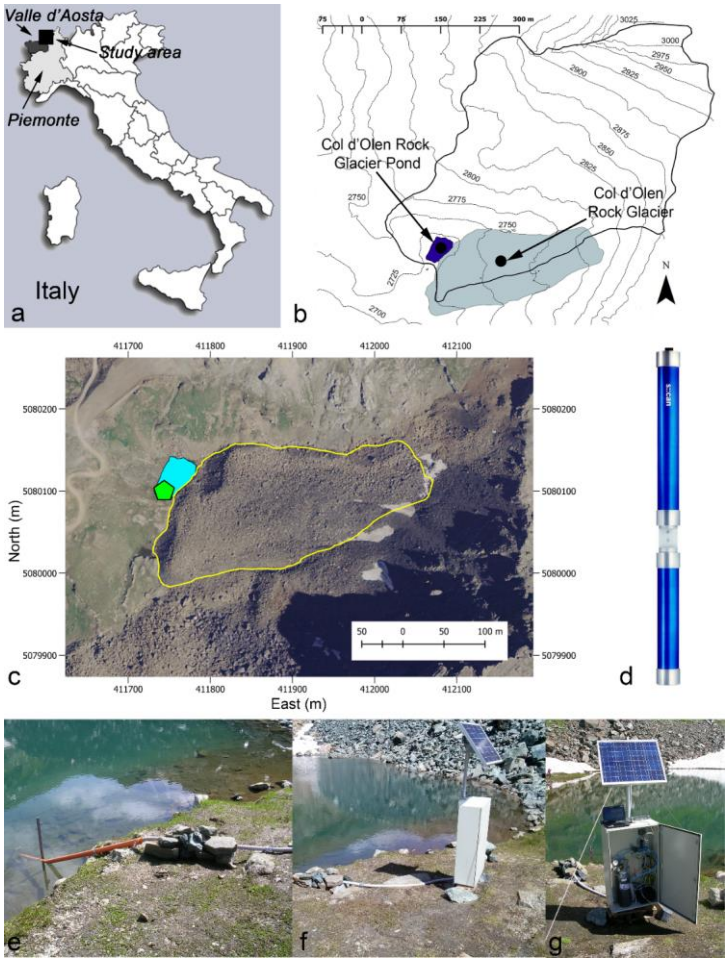

Figure 1. (a) Location of the study area in Italy. (b) Elevation map of the study area showing the extent of the catchment, the Col d'Olen Rock Glacier, and the Col d'Olen Rock Glacier Pond. (c) Aerial view of the Rock Glacier Pond system and location of the UV–Vis probe (green polygon) on the southern side of the pond (cyan polygon) (aerial image year 2006, coordinate system WGS 84 / UTM zone 32N). (d) Image of the probe used in this study. Details of the probe installation site: (e) installation in the pond, (f) on-shore installation with electrical and solar panels, and (g) internal view of the electrical panel, with pressurised air system and battery.

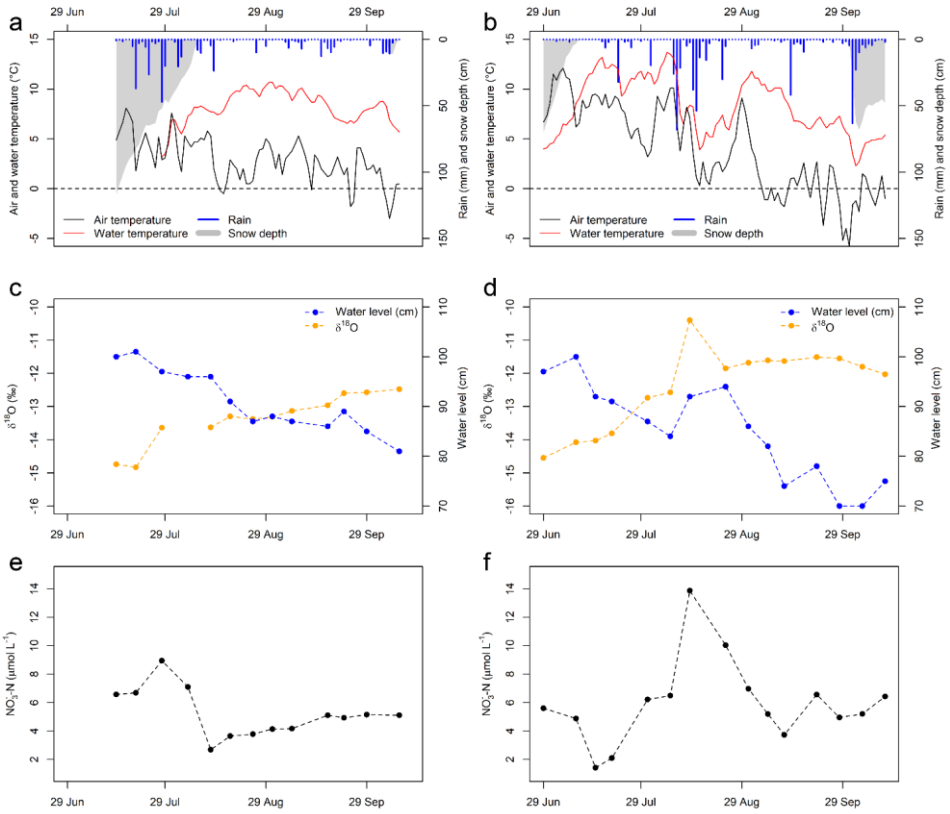

Figure 2. Daily air temperature, water temperature, rain, and snow depth in (a) 2014 and (b) 2015. Water level and $\delta^{18}O$ values in grab samples in (c) 2014 and (d) 2015 (only $\delta^{18}O$ is shown given the high correlation with $\delta^{2}H$). NO_3^--N concentrations in grab samples in (e) 2014 and (f) 2015.

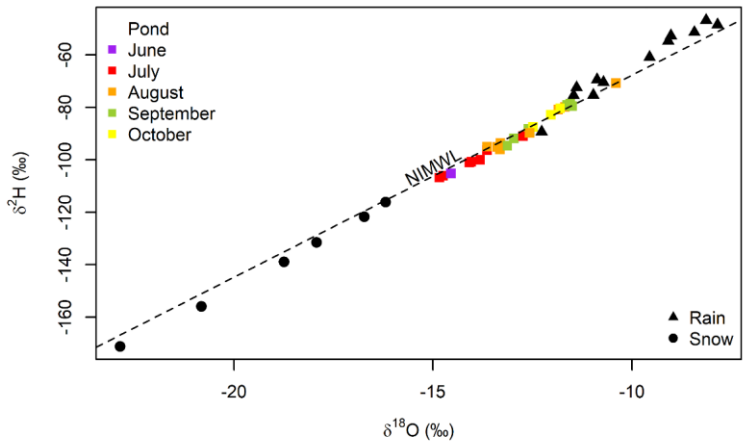

Figure 3. Dual-plot isotope distribution showing pond, snow and rain data. For pond samples, different colours identity the sampling months (from June to October). NIMWL: Northern Italian Meteoric Water Line.

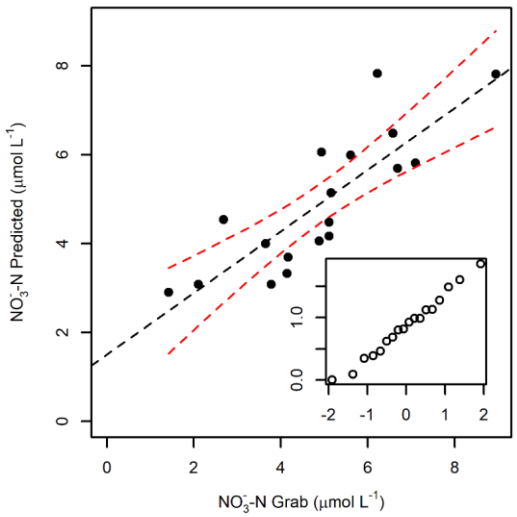

912

913 Figure 4. Scatterplot of grab samples against the values predicted by the linear regression model
914 with confidence levels at 95 % (n = 18, r = 0.83, $p < 0.01$). The inset shows the normal quantile-
915 quantile plot of residuals of the final regression model (x axis: theoretical quantiles; y axis: residual
916 quantiles).

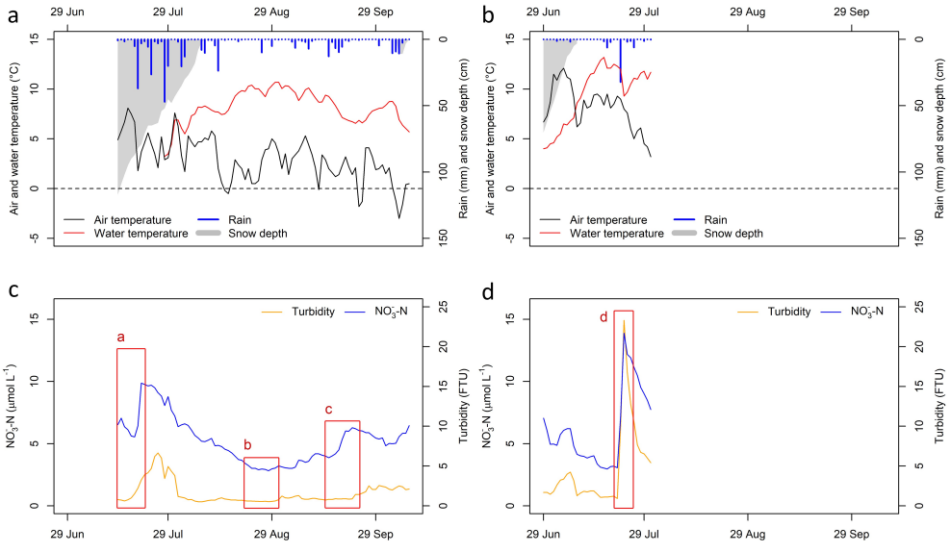

Figure 5. Daily air temperature, water temperature, rain, and snow depth in (a) 2014 and (b) 2015 (meteoclimatic conditions are shown in Fig. 2 and here to enhance the interpretation of the NO_3^--N and turbidity variations measured by the probe). Daily NO_3^--N concentrations and turbidity estimated by the probe in (c) 2014 and (d) 2015. Red windows in panels c and d refer to panels a–d in Fig. 6.

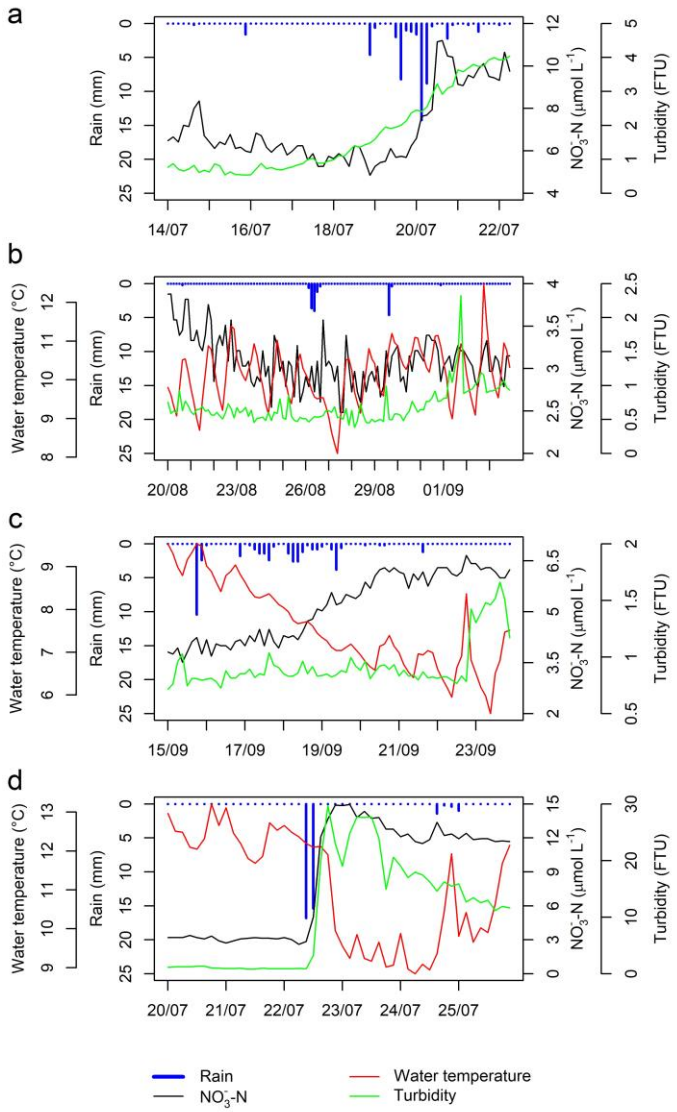

923

924 Figure 6. Three-hourly rain, water temperature (when available), and NO_3^--N concentrations and
925 turbidity estimated by the probe in four selected periods: (a) 14 – 22 July 2014 (water temperature
926 was not measured in this period), (b) 20 August – 3 September 2014, (c) 15 – 23 September 2014,
927 and (d) 20 – 25 July 2015.